Sensors and Actuators Reports 9 (2025) 100324

Contents lists available at ScienceDirect

Sensors and Actuators Reports

journal homepage: www.sciencedirect.com/journal/sensors-and-actuators-reports

Ultra-sensitive aptameric field-effect transistor for cortisol sensing

Thi Thanh Ha Nguyen [a,b,1], Cong Minh Nguyen [a,c,1], Minh Anh Huynh [a,b], Quang Thang Trinh [a], Philip Tanner [a], Sven Ingebrandt [d], Xuan Thang Vu [d,*], Tuan-Khoa Nguyen [a,*], Nam-Trung Nguyen [a,*]

[a] Queensland Micro- and Nanotechnology Centre, Griffith University, Nathan, QLD 4111, Australia
[b] School of Engineering and Built Environment, Griffith University, Nathan, QLD 4111, Australia
[c] School of Environment and Science, Griffith University, Nathan, QLD 4111, Australia
[d] Institute of Materials in Electrical Engineering 1, RWTH Aachen University, Sommerfeldstr. 24, Aachen 52074, Germany

ARTICLE INFO

Keywords:
Field effect transistor
Aptamer
FET sensor
Cortisol
Body fluids
Lab on chip
Point of care

ABSTRACT

Existing diagnostic methods for major depressive disorders, emerging mental disorders globally, are restrictive and inaccurate due to the lack of evidence-based assessments. Recent developments incorporating advanced material, micro/nano manufacturing and biology enable new clinical pathways using biosensors that can provide new opportunities for the diagnosis of mental condition from an early developmental stage. In this work, we present an ultra-sensitive lab-on-chip biosensor platform that is capable of detecting cortisol, a key biomarker for depression in physiological fluid. Utilizing advanced microfabrication techniques, our biosensor achieves a compact footprint of 5.0 mm by 2.5 mm, making it suitable for integration into portable and wearable devices. The device exhibits an ultra-low detection limit of 1 fM and a wide dynamic detection range spanning from 1 fM to 1 μM, covering the concentration present in physiological body fluids of human. Our finding shows a great potential for the development of accurate, and point-of-care monitoring system for early detection of depression disorders to advance the mental health diagnosis.

1. Introduction

Major depressive disorders (MDDs) are among the most prevalent mental health conditions worldwide, affecting approximately 264 million people globally [1]. MDDs are typically characterized by persistent depression, low energy, and loss of interest in daily activities, and if left undetected and untreated, they can potentially lead to suicidal tendencies [2]. The alarming emergence of MDDs in the population not only affects individual quality of life, but also poses significant societal challenges and burdens to healthcare systems globally with respect to diagnosis and treatment [3].

Diagnosing MDDs, especially in their early stage, remains challenging due to its reliance on subjective methods such as interviews and self-assessments instead of evidence-based assessments utilizing objective biochemical indicators [4]. Among various biomarkers for MDDs, cortisol, called stress hormone, stands out as one of the most prominent biomarkers for the diagnosis of depression [5]. However, cortisol typically presents at low levels in physiological fluids and varies dynamically due to daily activities and individual health conditions. Fig. 1A briefly summarizes the release mechanism of cortisol by the adrenal gland during psychological or physical stress. A period of stress activates the hypothalamic-pituitary-adrenal axis, which starts with the overproduction of corticotropin-releasing hormone (CRH). This excess CRH leads to a heightened release of adrenocorticotropic hormone (ACTH) from the anterior pituitary, prompting the adrenal glands to secrete an increased level of cortisol [6,7]. Cortisol dysregulation is usually observed in major depressive disorders, anxiety disorders, posttraumatic stress disorders, obesity, as well as Cushing's and Addison's diseases [2]. Therefore, deficiency, excess, or irregular patterns of cortisol are evidently associated with mental disorders [5].

Over the past decade, a great deal of research has been dedicated to the development of cortisol detections in physiological fluids such as blood, saliva, sweat, hair, urine, and interstitial fluids [8–10]. Nevertheless, the accurate and continuous monitoring of cortisol concentration remains challenging due to difficulties in sample collections (*e.g.*, invasiveness of collecting blood samples, inconvenience of taking urine

* Corresponding authors.
E-mail addresses: vu@iwe1.rwth-aachen.de (X.T. Vu), k.nguyentuan@griffith.edu.au (T.-K. Nguyen), nam-trung.nguyen@griffith.edu.au (N.-T. Nguyen).
[1] TTHN and CMN contributed equally to this work

https://doi.org/10.1016/j.snr.2025.100324
Received 22 February 2025; Received in revised form 31 March 2025; Accepted 2 April 2025

samples), transport and storage in lab-based methods [10]. Moreover, conventional clinical methods such as enzyme-linked immunosorbent assay and gas chromatography-mass spectrometry utilize labelling and/or bulky equipment for extraction and detection of biomarkers from body fluids, making them unsuitable for decentralized healthcare systems [11,12]. Therefore, it is demanding to develop healthcare systems for monitoring of cortisol levels to quantitatively analyze stress levels for early detection of MDDs.

Recently, lab-on-chip biosensors have been utilized to address the need for non-invasive monitoring of physiological data and detection of early biomarkers, offering valuable insights into the performance and health of individuals [5,10,13–18]. The integration of bio recognition elements into these sensors potentially enables the management of chronic conditions and facilitates remote monitoring [19–23]. Among these sensing platforms, biologically sensitive field-effect transistors (bio-FETs) have attracted significant attention from the research community for their rapid response, label-free detection, ultra-sensitivity, broad dynamic range, low power operation, miniaturization, and cost-effective fabrication processes [5]. These sensors can be implemented on flexible substrates, surpassing the abilities of other existing methods [24,25], making bio-FET one of the most promising candidates for wearable systems. Despite their advancements, current lab-on-chip technologies face limitations in adequately limit of detection (LOD) and continuous measurement that are essential for accurate and real-time diagnosis of MDDs. We recently developed different types of bio recognition sensors that can push the LOD of various bio molecules to ultra-low levels for point-of-care early detection of diseases [26–28].

Capturing probes, including molecularly sensitive polymers, antibodies, and aptamers have been employed for cortisol detection [29–31]. Among these probes, aptamers, which are nucleic acid molecules folding into structures tailored for their specific target molecules, offer significant advantages for bio-FET devices [10]. First, aptamers demonstrate exceptional affinity and selectivity, serving as adaptable receptors capable of binding specifically to their targets [32]. Second, aptamers carry negative charges due to the phosphate group in each nucleotide, enabling binding of the target to cause change in surface potential of the FET [10]. Third, aptamers are smaller than antibodies, minimizing the risk of surpassing the Debye length during target binding process. Moreover, aptamers can be chemically synthesized *in vitro* at a low cost and minimal batch-to-batch variability [10,33]. Aptamers also exhibit greater resistance to temperature fluctuations and demonstrate superior long-term stability [34,35]. Different aptamers have been introduced for cortisol detection, with the length of 40 [36], 61[37], 85 [31,38] and 44 [15] nucleotides. Notably, the one with 44 nucleotides has been previously employed in a FET sensor for cortisol detection with LOD down to 1 pM [15].

In this work, we present a miniaturized, ultra-sensitive biosensor, which assist the diagnosis of depression by detecting pH change and cortisol variation in PBS 0.01X, using an ion-sensitive field-effect transistor (ISFET) platform, Fig. 1B After bio-functionalization with aptamer, the resultant LOD for cortisol was found to be 1 fM, with a dynamic range spanning 9 orders of magnitude, covering the range of clinical samples. To our best knowledge, the LOD of our device is the lowest detection limit reported to date in literature, offering stability for cortisol sensing in physiological fluids, Fig. 1C. The present ISFET-based biosensor utilizes a small sample volume, is label-free and shows excellently broad dynamic range and high sensitivity.

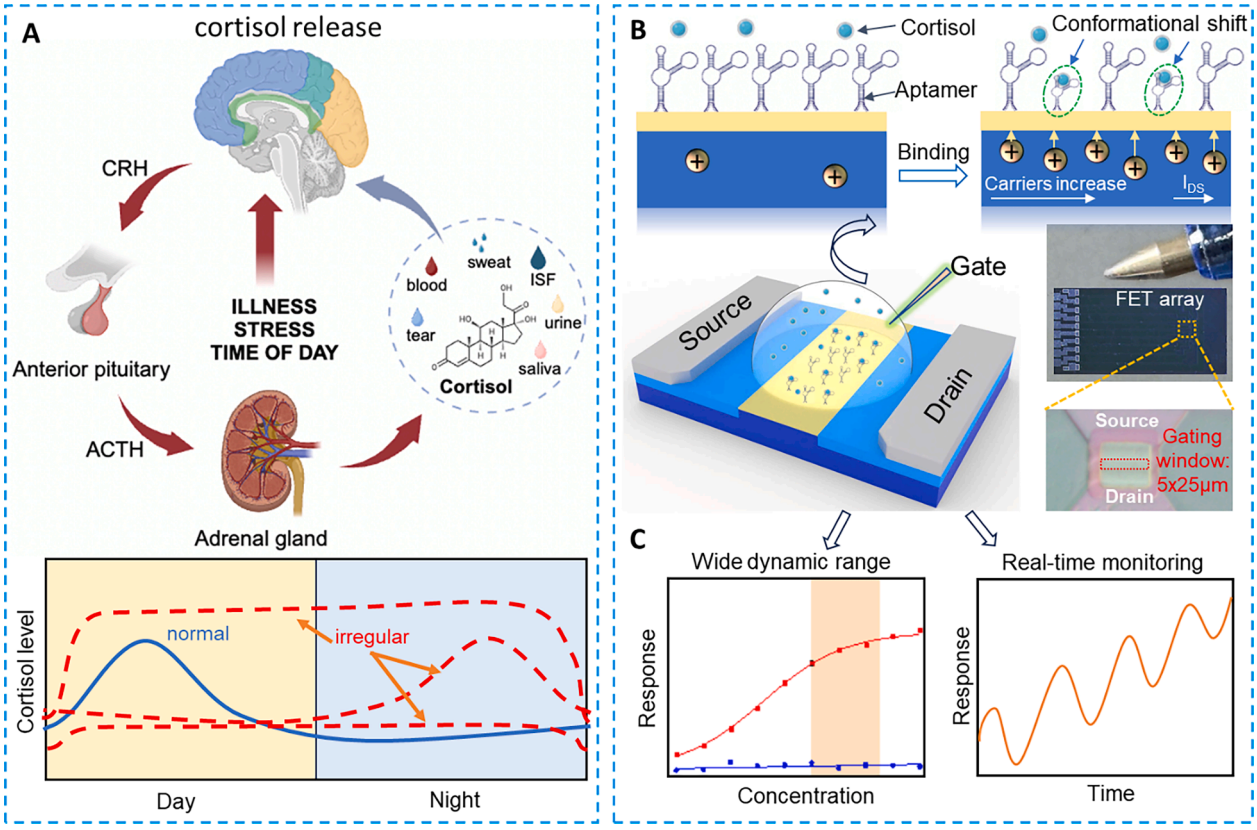

Fig. 1. Conceptualization of ISFET for major depressive disorders (MDDs) diagnosis. (A) Cortisol released mechanism during MDDs (CRH: Corticotropin-releasing hormone, ACTH: Adrenocorticotropic hormone). (B) Design of aptamer-functionalized ISFET cortisol biosensor in this work, binding of target to aptamer results in a negative top-gating effect on the sensing channel, generating a measurable change in the drain-source current. *(Note: Figure not drawn to scale).* (C) Concept of cortisol detection with the current biosensor for MDDs diagnosis.

2. Materials and methods

2.1. Materials

All chemicals were purchased from Sigma-Aldrich Co. (St. Louis, MO) unless otherwise noted. Thiolated cortisol aptamer and scramble control were synthesized by Integrated DNA Technologies (IDT, Coralville, IA). Detailed aptamer oligo sequence is 5′-/5ThioMC6-D/ CGA CTG GTA GGC AGA TAG GGG AAG CTG ATT CGA TGC GTG GGT CG-3′ [15]. This sequence, developed through the systematic evolution of ligands by exponential enrichment (SELEX) by Wang et al., has been validated using a fluorescent assay [15]. The assay confirmed the aptamer's high affinity, with a dissociation constant (K_d) of 500 nM in solution and an enhanced Kd of 30 pM on a FET platform [15]. This aptamer has negligible binding to non-specific targets relevant in physiological fluids, such as progesterone, testosterone and serotonin [15]. Scramble sequence is 5′-/5ThioMC6 D/ CCA CCG CAG TCC GGT CGC TTG CTC GCT GTG TGG GTA GTA GGT CG-3′, which has similar length and GC content as the aptamer sequence [15].

2.2. Device fabrication

The FET device fabrication was adapted from our previous work [39]. Briefly, 1-μm layer of silicon oxide was grown on a 4-inch n-type silicon wafer using a wet oxidation. Next, the contact interconnects were formed by doping with boron for open-gate ISFETs (Supplemental Fig. S1). Boron implantation was applied to the contact lines at a dose of 1×10^{16} ions/cm^2, 150 keV. A shallow boron implantation (1×10^{15} ions/cm^2, 80 keV) was performed to define the source and drain contacts. The source and drain contact patches were fabricated using a lift-off process with an Al/Ti/Au metal stack. Following this, the implantation oxide was then entirely removed, and a 220 nm-thick SiO_2 was grown via a wet oxidation process to serve as a device passivation. Next, lithography was carried out to open window contacts for the source/drain/gate. Subsequently, a 6 nm-thick SiO_2 was thermally grown in a dry oxidation process at 820 °C to passivate the sensing area. To finalize the fabrication, outer source/drain contacts were produced through another lift-off process using the similar Al/Ti/Au stack. 1 % hydrofluoric acid was used to etch the SiO_2 layer to open the source/-drain contact areas. In our process,multiple wafers were fabricated using identicial parameters within the same batch. The ISFET characterization after chip fabrication showed that transistors with the same parameters exhibit identical characteristics in all wafers.

2.3. FET bio-functionalization

The ISFET semiconductor surface was functionalized with (3-Aminopropyl)triethoxysilane (APTES), self-assembled through vapor-phase deposition via a salinization process. First, SiO_2 surface was treated with UV Ozone (Ossila, Ltd., UK) for 5 min for cleaning and maximizing hydrophilicity (Supplemental Fig. S2). Next, APTES solution and devices were placed in a vacuum chamber at 80 °C for 1 h, followed by an additional hour of baking at the same temperature. The APTES molecule features a group that covalently binds to gate oxide and an amine group at the other end, which can react further with linker m-Maleimidobenzoyl-N-hydroxysuccinimide ester (MBS). Silanized FETs were rinsed with ethanol and DI water, then immersed in 1 mM MBS dissolved in a 1:9 (v/v) mixture of dimethyl sulfoxide (DMSO) and PBS (pH 7.4) for 30 min. These linkers introduce functional groups that can covalently bind to thiol-containing aptamers. The aptamers were immobilized by applying a 10 μL drop of 10 μM thiolated DNA aptamer solution overnight, followed by rinsing with deionized water and dried under N_2 gas. The thiol group at the 5′ end of the aptamers cross-linked with the amine-terminated silanes via MBS.

2.4. Water contact angle measurement

Sessile drop contact angle measurements were carried out under ambient conditions, using an optical tensiometer (Theta Flex, Biolin Scientific, Finland). A micro syringe was used to dispense 5 μL drops of deionized water at multiple locations across the substrate surface. The image capture system captured droplet images every 0.1 s. The surface tension was determined by rapidly collecting droplet images, performing edge detection, and fitting them to the Laplacian–Young equation. The ambient temperature for all analyses was 25 °C.

2.5. X-ray photoelectron spectroscopy (XPS)

XPS was employed to confirm the successful binding of chemicals at each functionalisation step on the semiconductor surface. The XPS spectra were acquired using an AXIS Supra plus photoelectron spectrometer (Kratos Analytical, UK), with monochromatic Al Kα X-rays (1486.6 eV) as the incident radiation, operating at 100 W (10 kV, 10 mA). Vacuum-dried samples were scanned across a binding energy range of 1200-0 eV using an analyzer pass energy of 160 eV with 1.0 eV steps and a scan duration of 120 s. For narrow high-resolution (HR) scans, a pass energy of 20 eV, 0.1 eV steps, and a scan duration of 60 s were used, with up to 5 sweeps per HR scan. The base pressure in the analysis chamber during the measurements was maintained below 10^{-8} Torr.

2.6. Atomic force microscopy (AFM)

AFM was employed to examine the surface morphology of SiO_2 to ensure surface homogeneity after immobilization. Atomic force microscopy (AFM) images were captured with a Dimension Icon AFM (Bruker). Imaging was conducted in air using ScanAsyst in Air Mode with ScanAsyst-Air probes (Bruker). The AFM scan rate was 1 Hz, 256 samples per line and a scan size of 0.5 μm × 0.5 μm. Image processing steps, such as row alignment, horizontal scar correction, and height scale adjustment, were completed using a NanoScope Analysis (version 2.0, Bruker).

2.7. Spectroscopic ellipsometry

Ellipsometry was used to measure the thickness of sensing layers. The samples were measured using a Variable Angle Spectroscopic Ellipsometer, and the results were calculated using WVASE32® software. The thickness of the native SiO_2 and silane layer was determined for bare silane-modified silicon substrates and was taken as a constant to fit the thickness of the aptamer layer.

2.8. Electrical measurement of pH and cortisol

All electrical measurements were conducted using a Keithley B2600 SMU workstation. The solution was applied to the sensing channel then the drain current was measured when applying the gate voltage from Ag/AgCl reference electrode (SD5; World Precision Instruments Inc., Sarasota, FL) for the characterization of the sensing device. Transfer curves were recorded by varying the gate voltage (V_{GS}) from 0.0 to −3.0 V for pH sensing and from 0.0 to −2.0 V for cortisol sensing, with steps of −20 mV. For pH sensing, ISFET was immersed in pH buffer solutions ranging from 3 to 11 (Sigma Aldrich). The device operated in a three-terminal configuration, consisting of the source, drain, and gate. Calibrated responses were determined based on the transfer curve results.

For cortisol sensing, the sensing area of the ISFET was incubated with cortisol solutions ranging from 1 fM to 1 μM in 0.01X PBS. For each target or non-target concentration, three overlapping transfer curves were averaged.

3. Results and discussion

3.1. Characterization of ISFETs and pH sensing

Electrical performance of the fabricated ISFETs was characterized using an Ag/AgCl reference electrode for solution gate biasing in phosphate-buffered saline (PBS), Fig. 2A. Fig. 2B presents the output characteristics of a device obtained by scanning the drain-source voltage (V_{DS}) from 0.0 to −3.0 V while stepping the gate voltages (V_{GS}) from 0.0 to −3.0 V (500 mV steps). We observed an increasing drain current (I_{DS}) as a response to negative V_{GS}. These characteristics are typical of p-channel enhancement mode ISFET [40]. Fig. 2C and D show the transfer characteristics of the device, indicating a sub-threshold swing (SS) value of approximately 200 mV/dec. From the transconductance curve of the device, the threshold voltage (V_{th}) value was determined to be 0.33 ±0.03 V, Fig. 2E. This low threshold voltage makes our ISFET suitable for applications requiring low power consumption such as wearable devices. Typical leakage current was measured to be in sub-nA (Supplemental Fig. S3), confirming the high quality of the fabricated structures that are suitable for liquid measurement in biosensing.

We first evaluated our ISFETs as pH sensors for a pH range from 3 to 11 (Fig. 2F), which fully covers the physiological pH variation in human sweat. The detection mechanism can be detailed as follow. Upon contact with an aqueous solution, the oxide surface of ISFET gate can be hydrogenated to form hydroxyl group (OH-), enabling the device to serve as a pH sensor. Depending on the pH level, these hydroxyl groups can either protonate or deprotonate, causing the surface potential alternation of the ISFET sensor (Fig. 2A inset). Fig. 2F shows that at a high pH level, the hydroxyl groups are protonated, enhancing the gate effect and increasing the drain current. Conversely, at a low pH level, the hydroxyl groups are deprotonated, weakening the gate effect and reducing the drain current.

We derived the threshold voltage (V_{th}) value for the ISFET sensor based on the transconductance extrapolation method [41]. Briefly, the threshold voltage corresponds to the intercept of the gate voltage axis with the linear extrapolation of the gm–Vg characteristics at its maximum first derivative point. Calibrated responses were determined by calculating the shift in threshold voltage (ΔV_{th}), accounting for baseline subtraction through changes in the source−drain current. Fig. 2G indicates a highly linear response to the pH range from 3.0 to 9.0 ($R^2 = 0.9973$), with a pH sensitivity of 20.3 mV/pH.

The device was readily responsive for real-time pH monitoring, Fig. 2H. The pH sensor responded instantly and generated current signal after replacement of the pH buffers. The observed response time was below 5 s, demonstrating the fast response of the ISFET to pH changes.

3.2. Bio-functionalization and surface characterization for cortisol sensing

Capturing probes, including molecularly sensitive polymers, antibodies, and aptamers have been employed for cortisol detection [29–31]. Among these probes, aptamers, which are nucleic acid molecules folding into structures with binding pockets tailored for their specific target molecules, offer significant advantages for bio-FET devices [10]. First, aptamers carry negative charges due to the phosphate group in each nucleotide, enabling binding of the target to cause a change in surface potential of the FET. Second, aptamers are smaller than antibodies, minimizing the risk of surpassing the Debye length during target-binding process. Moreover, aptamers can be chemically synthesized *in vitro* at a low cost and minimal batch-to-batch variability.

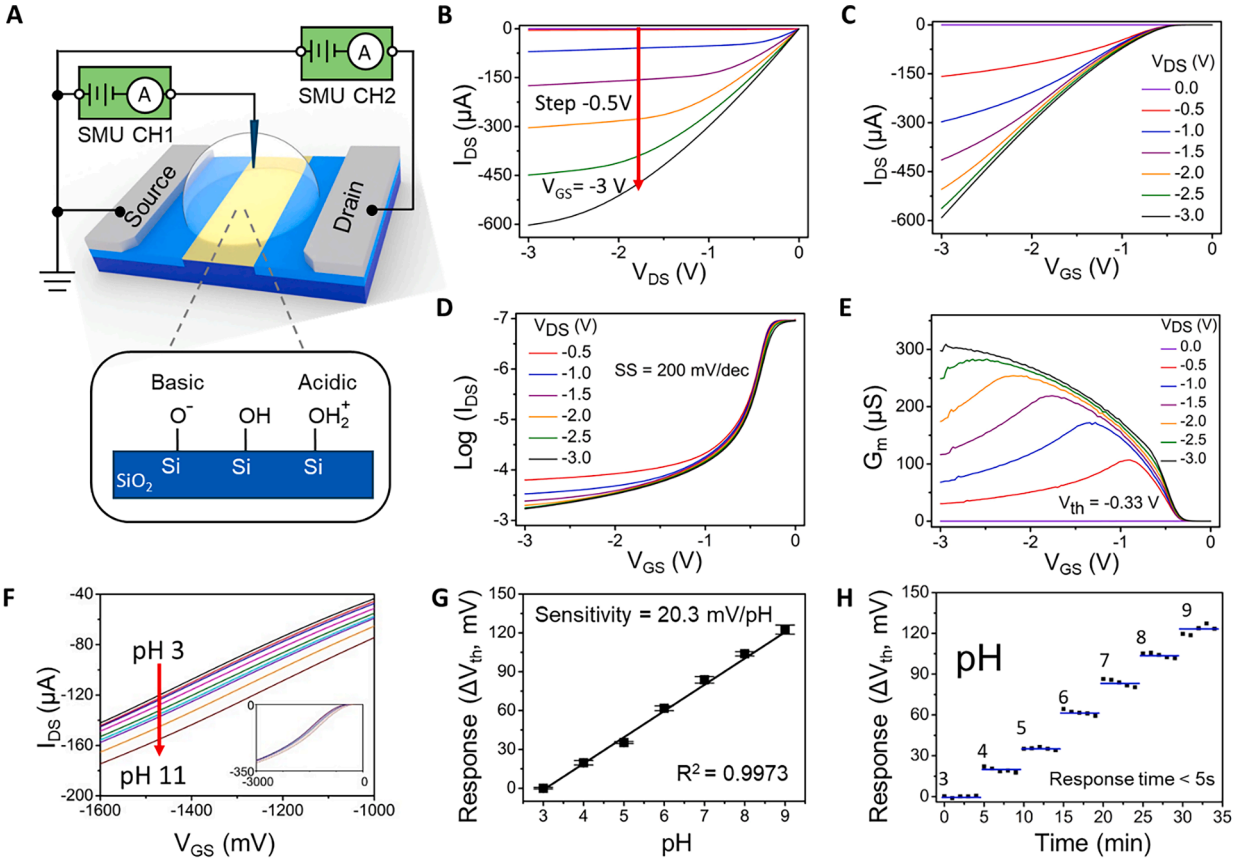

Fig. 2. Electrical characterization and pH sensing. (A) Representative illustration of ISFET as pH sensor *(Note: Figure not drawn to scale),* (B) output curve, (C) transfer curve (linear scale), (D) transfer curve (semi-log scale) showing subthreshold swing (SS) value, (E) transconductance curve, (F) drain currents at different pH levels, (G) pH calibration curve ($N = 5$ devices), (H) real-time pH sensing of a device with sequential incubation of increasing pH over time.

Aptamers also exhibit greater resistance to temperature fluctuations and demonstrate superior long-term stability. Different aptamers have been introduced for cortisol detection, with the length of 40 [36], 61[37], 85 [31,38] and 44 [15] nucleotides. Notably, the one with 44 nucleotides has been previously employed in a FET sensor for cortisol detection with LOD down to 1 pM [15].

To create an aptamer-FET sensing interface, a thiolated cortisol aptamer was covalently immobilized to amino-silanized ISFET channels utilizing 3-maleimidobenzoic acid N-hydroxysuccinimide ester (MBS) as the cross-linker, as illustrated in Fig. 3A. The cortisol-specific aptamer sequence used in this study was demonstrated as an effective receptor for binding cortisol to the sensing surface [15].

We measured the apparent water contact angle (WCA) to characterize the change in wetting behavior of the surface after the functionalization process. Fig. 3B–E show the water contact angle measurements for the SiO_2 surface at different stages of functionalization. The bare surfaces have a contact angle of 74.1°± 0.4°, indicating that the material is lightly hydrophilic in its native state. The treatment with UV-Ozone significantly reduces the contact angles to 8.5°± 0.7°, indicating that UV-Ozone treatment made the surface super-hydrophilic, which is consistent with the introduction of polar groups (*i.e.*, hydroxyls) onto the surface. The functionalization with APTES, which contains amino group ($-NH_2$) makes the surface more hydrophilic compared to the bare surface. The presence of the $-NH_2$ group can form hydrogen bonds with water molecules, thus reducing the WCA to 61.3°±2.6° The aptamers are likely to present a more hydrophilic sugar-phosphate backbone to the surface than APTES alone, leading to a lower WCA of 43.4°± 0.2°.

Atomic Force Microscopy (AFM) was utilized to examine the morphology of SiO_2 surface to ensure the homogeneity after immobilization. Fig. 3F–I show the root mean square (RMS) roughness value of bare SiO_2 surface as 0.22±0.01 nm. After the salinization step (see Method section), the RMS roughness significantly increased to 0.68

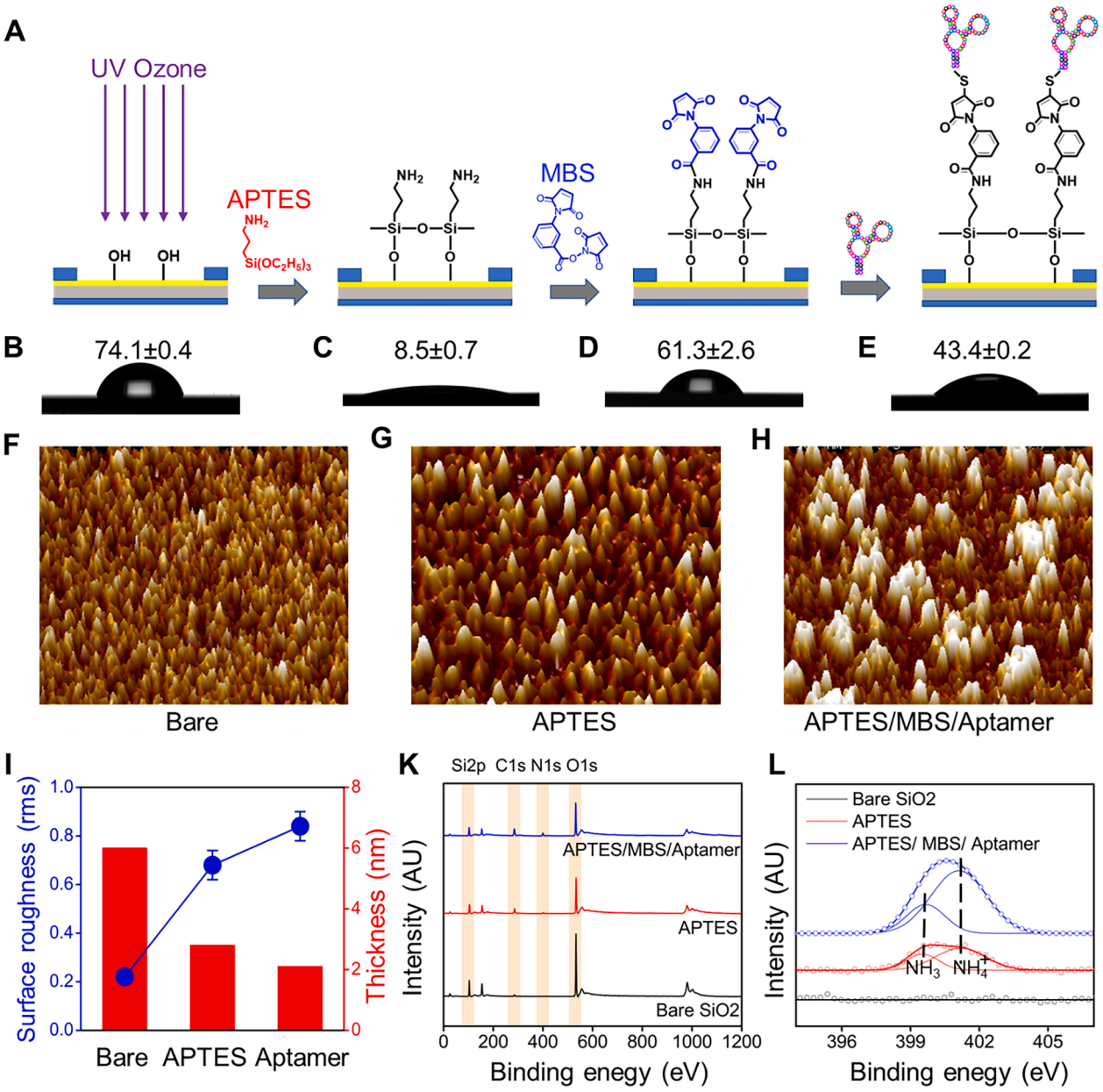

Fig. 3. Bio-functionalization of ISFET for cortisol detection. (A) Illustration of bio-functionalization strategy *(Note: Figure is not drawn to scale),* (B–E) water contact angles of untreated, UV-ozone-treated, APTES-deposited, and aptamer-immobilized SiO_2 surfaces, (F–H) AFM topographical scans of untreated, APTES-deposited, and aptamer-immobilized SiO_2 surfaces, (I) Root mean square surface roughness (rms) analysis from AFM and layer thickness analysis from spectroscopic ellipsometry, (K–L) Full scan and high-resolution N1s scan with XPS analysis.

±0.06 nm, indicating that the APTES layer adds topographical features to the surface, which is expected with the molecules attached to the surface. After further functionalization with aptamer, the RMS roughness values increased to 0.84±0.06 nm. The further increase of roughness suggests that the aptamer, being a structurally larger and more complex biomolecule compared to APTES, contributes to a more pronounced surface topography.

The thickness of functionalized APTES and aptamer layers was analyzed with spectroscopic ellipsometry (see Method section). Fig. 3I indicates that the thickness of the APTES layer was 2.8 nm, suggesting 2 to 3 layers of molecules were deposited on the sensing surfaces. The thickness of the aptamer layer is 2.1 nm, which is consistent with the typical aptamer sizes [42].

The presence of elemental composition in the surface of silicon was measure by X-ray photoelectron spectroscopy (XPS). In the full scan (Fig. 3K), the Si, C, N, O elements in ~100, 300, 400 and 500 eV regions can be observed, respectively. As shown in the high-resolution N1s scan (Fig. 3L), successful APTES functionalization and aptamer immobilization were confirmed by the presence of nitrogen (binding energy of approximately 400 eV) on the sensor surface after functionalization. The amount of nitrogen increases further after the immobilization of aptamer. Interestingly, in both case of APTES functionalization and aptamer immobilization, N1s peaks were dominantly composed of NH_4^+ oxidation state over NH_3 species.

Supplemental Fig. S4 compares the transfer characteristic curves of the bare ISFET, after APTES modification, and after aptamer immobilization. After APTES functionalization, there was a shift in transfer curves, indicating the successful introduction of amino-silane groups on the gate dielectric surface, which alters the interfacial charge distribution. Further immobilization of the aptamer results in a more pronounced shift in drain currents, reflecting the additional surface charge and dipole effects introduced by the aptamer molecules. These shifts in the transfer characteristic curves highlight the sensitivity of the ISFET to surface modifications, confirming that each step in the functionalization process contributes to the final electrical response of the biosensor.

3.3. Cortisol sensing

We investigated the capability of the ISFET biosensor for detection of cortisol by its response to varying cortisol concentrations in 0.01X PBS solution, Fig. 4A. During the tests, the gate voltage (V_{GS}) was swept from 0.0 to −2.0 V in −0.02 V-steps, while the drain-source voltage (V_{DS}) was held constant at −1.0 V. Fig. 4B shows the raw drain-source current for various cortisol concentrations, ranging from 1 fM to 1 μM. The transfer curves exhibit a clear rightward shift of I_{DS} with increasing cortisol concentration. In the absence of the target, the immobilized aptamer on the sensing surface remains in a flexible, looped, and unfolded configuration. Upon capturing cortisol, the aptamer undergoes conformational changes, where its negatively charged phosphodiester backbone attached to the sensing channel surface adopts a more compact

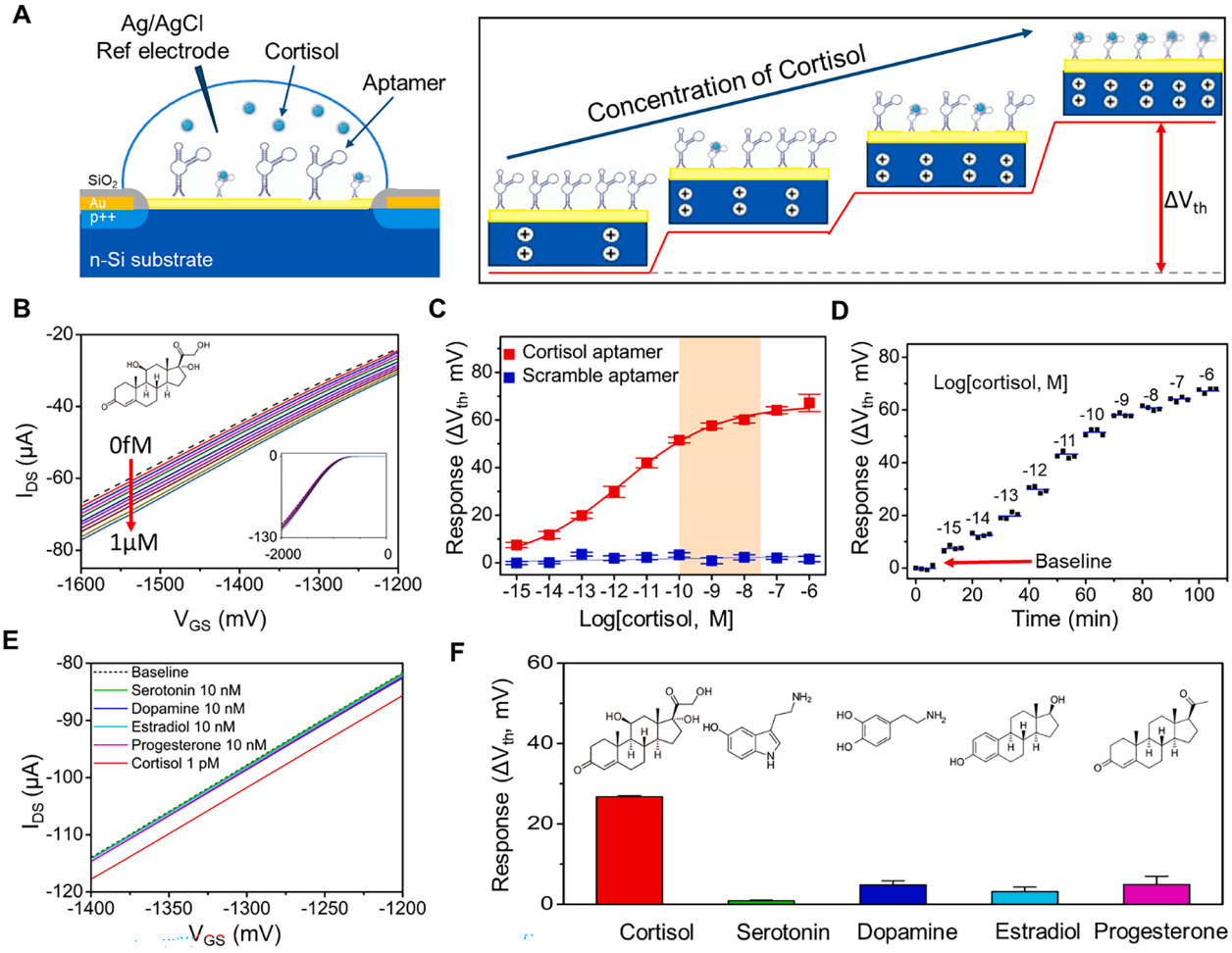

Fig. 4. Cortisol sensing with aptamer-functionalized ISFET. A) Schematic illustration of aptamer-functionalized ISFET for cortisol sensing. *(Note: Figure is not drawn to scale)* (B) Transfer curves, (C) Calibrated responses (shaded area represents clinical range) ($N = 5$ devices), (D) Cortisol sensing in 0.01X PBS buffer of a device with sequential incubation of increasing cortisol concentrations over time, (E) Comparison of dynamic range of recent cortisol sensing platforms, (F) Specificity of aptamer-functionalized ISFET against 10 nM serotonin, dopamine, estradiol and progesterone. The device produced minimal response compared to 1 pM cortisol.

structure. This structure channels the negative charges closer to the sensing surface, resulting in a negative top-gating effect, which in turn generates a measurable change in the drain-source current [10].

Calibrated responses were determined by calculating the shift in threshold voltage (ΔV_{th}) in a similar manner as pH calibrated response. Calibration curve in Fig. 4C shows a non-linear relationship with cortisol concentration before reaching saturation, which agreed with previous studies [15,43–45]. The physiological range of sweat cortisol falls within the experimental range used in this study. Additionally, the ISFETs were functionalized with scrambled aptamers to account for non-specific binding. The modified chips were incubated with cortisol during the measurements. The results indicated that the scrambled aptamers showed no significant response on these chips.

We tested the capability of our device to sequentially respond to different concentrations of cortisol from 1 fM to 1 μM. As shown in Fig. 4D, the aptamer-functionalized device was able to respond within 5 min of incubation, producing a stable reading throughout the assay. It is well-known that ISFET sensors could exhibit an instability and monotonic temporal changes in the threshold voltage of the device [5,46,47]. This is crucial for designing an accurate sensor to produce a stable, drift-independent response. Supplemental Fig. S5 indicates that the drift in threshold voltage of our devices was quasi-negligible. Therefore, we conclude that any potential drift influence is minor for our aptamer-functionalized ISFET.

In a control experiment, our device displayed minimal responses to 10 nM serotonin, dopamine, estradiol, progesterone as compared to 1 pM cortisol (Fig. 4E and F). This result demonstrates that the ISFET sensor exhibits excellent selectivity characteristics for cortisol detection, which prevents unwanted binding and crosstalk signal. To our best knowledge, to date our device exhibited the lowest LOD while offering widest dynamic range for cortisol sensing (Supplemental Table S1).

4. Conclusion

In summary, we successfully demonstrated an ultra-sensitive and miniturized ISFET sensor using micro technology for the sensing of cortisol hormone, which is essential for assessing stress and depression development from an early stage. We employed surface functionalization with aptamer as the bio-probe to achieve ultra-high sensitivity, excellent selectivity, and stability. Surface characterization using XPS, AFM, water contact angle and ellipsometry confirmed the presence of chemical elements on the sensing area, indicating the successful immobilization of the aptamer to the sensing surface. The bare sensor can monitor pH level from 3 to 9, which fully cover the pH range of physiological fluid with good linearity and sensitivity. Furthermore, the aptamer-functionalized ISFET sensor detected cortisol with an extremely low limit of detection (LOD) of 1 fM in 0.01X PBS and spanning a wide detection range of up to 1 μM. This unique low LOD makes it a promising candidate for detecting either normal or abnormal cortisol levels in biological fluids such as sweat with low sample volume, wide dynamic range, high sensitivity and selectivity.

We believe our platform could provide a feasible solution for lab-on-chip and point-of-care applications of other biomarkers such as serotonin, dopamine, and neuropeptides, opening a new avenue for sensitive wearable biosensors for health monitoring. Future work will focus on validating the sensor's performance in biological samples such as sweat, addressing challenges such as interference, signal drift, and reusability. Additionally, we will explore integration with microfluidic system to develop a compact, monolithic wearable device to ensure robust performance under physiologically relevant conditions.

Ethics approval and consent to participate

Not applicable.

Consent for publication

Not applicable.

CRediT authorship contribution statement

Thi Thanh Ha Nguyen: Writing – original draft, Visualization, Validation, Methodology, Investigation, Formal analysis, Data curation. **Cong Minh Nguyen:** Writing – original draft, Visualization, Validation, Methodology, Investigation. **Minh Anh Huynh:** Methodology, Investigation. **Quang Thang Trinh:** Software, Investigation. **Philip Tanner:** Methodology. **Sven Ingebrandt:** Resources, Methodology. **Xuan Thang Vu:** Writing – review & editing, Methodology, Investigation, Conceptualization. **Tuan-Khoa Nguyen:** Writing – review & editing, Supervision, Methodology, Investigation, Conceptualization. **Nam-Trung Nguyen:** Writing – review & editing, Supervision, Resources, Investigation, Funding acquisition, Conceptualization.

Declaration of competing interest

The authors declare that they have no competing interests.

Acknowledgments

The authors acknowledge the facilities, the scientific and technical assistance, of the Microscopy Australia Facility at the Centre for Microscopy and Microanalysis (CMM), and Australian National Fabrication Facility (ANFF) Queensland Node at the University of Queensland. T.T.H. Nguyen was funded by Australian Academy of Technological Sciences and Engineering. M.C. Nguyen was funded by Griffith University Higher Degree Research Scholarship. N.T. Nguyen and M.A. Huynh acknowledge funding from Australian Research Council (ARC) Discovery Project (DP220100261) and Laureate Fellowship (FL230100023). T.K. Nguyen acknowledges the support from Australian Research Council DECRA Fellowship (DE240100408), DAAD Australia-Germany Joint Research Cooperation Scheme, and Griffith New Researcher Grant. X.T.Vu acknowledges DAAD Australia-Germany Joint Research Cooperation Scheme.

Supplementary materials

Supplementary material associated with this article can be found, in the online version, at doi:10.1016/j.snr.2025.100324.

Data availability

Data will be made available on request.

References

[1] S.L. James, et al., GBD 2017 Disease and Injury Incidence and Prevalence Collaborators, Global, regional, and national incidence, prevalence, and years lived with disability for 354 diseases and injuries for 195 countries and territories, 1990-2017: a systematic analysis for the Global Burden of Disease Study 2017, Lancet 392 (10159) (2018) 1789–1858.
[2] R.H. Belmaker, G. Agam, Major depressive disorder, New Engl. J. Med. 358 (1) (2008) 55–68.
[3] WHO, The Global Burden of Disease 2004, World Health Organization, 2008.
[4] X. Zhang, et al., Early-diagnosis of major depressive disorder: from biomarkers to point-of-care testing, TrAC Trends Anal. Chem. 159 (2023) 116904.
[5] S. Sheibani, et al., Extended gate field-effect-transistor for sensing cortisol stress hormone, Commun. Mater. 2 (1) (2021) 10.
[6] J.P. Herman, W.E. Cullinan, Neurocircuitry of stress: central control of the hypothalamo–pituitary–adrenocortical axis, Trends Neurosci. 20 (2) (1997) 78–84.
[7] S.M. Smith, W.W. Vale, The role of the hypothalamic-pituitary-adrenal axis in neuroendocrine responses to stress, Dialogues Clin. Neurosci. 8 (4) (2006) 383–395.
[8] R. Gatti, et al., Cortisol assays and diagnostic laboratory procedures in human biological fluids, Clin. Biochem. 42 (12) (2009) 1205–1217.
[9] A. Levine, et al., Measuring cortisol in human psychobiological studies, Physiol. Behav. 90 (1) (2007) 43–53.

[10] T.T.H. Nguyen, et al., Field effect transistor based wearable biosensors for healthcare monitoring, J. Nanobiotechnol. 21 (1) (2023) 411.
[11] J.H. Lee, et al., Emotion-on-a-chip (EOC): evolution of biochip technology to measure human emotion using body fluids, Med. Hypotheses 79 (6) (2012) 827–832.
[12] M. Debono, et al., Modified-release hydrocortisone to provide circadian cortisol profiles, J. Clin. Endocrinol. Metab. 94 (5) (2009) 1548–1554.
[13] M. Ku, et al., Smart, soft contact lens for wireless immunosensing of cortisol, Sci. Adv. 6 (28) (2020) eabb2891.
[14] R. Zhang, Y. Jia, A disposable printed liquid gate graphene field effect transistor for a salivary cortisol test, ACS Sens. 6 (8) (2021) 3024–3031.
[15] B. Wang, et al., Wearable aptamer-field-effect transistor sensing system for noninvasive cortisol monitoring, Sci. Adv. 8 (1) (2022) eabk0967.
[16] E.R. Kim, et al., Biosensors for healthcare: current and future perspectives, Trends Biotechnol. 41 (3) (2023) 374–395.
[17] M.Z. Li, S.T. Han, Y. Zhou, Recent advances in flexible field-effect transistors toward wearable sensors, Adv. Intell. Syst. 2 (11) (2020) 2000113.
[18] S.T. Han, et al., An overview of the development of flexible sensors, Adv. Mater. 29 (33) (2017) 1700375.
[19] A.J. Bandodkar, I. Jeerapan, J. Wang, Wearable chemical sensors: present challenges and future prospects, ACS Sens. 1 (5) (2016) 464–482.
[20] J. Heikenfeld, et al., Wearable sensors: modalities, challenges, and prospects, Lab Chip 18 (2) (2018) 217–248.
[21] G. Matzeu, L. Florea, D. Diamond, Advances in wearable chemical sensor design for monitoring biological fluids, Sens. Actuators B Chem. 211 (2015) 403–418.
[22] Y. Liu, M. Pharr, G.A. Salvatore, Lab-on-skin: a review of flexible and stretchable electronics for wearable health monitoring, ACS Nano 11 (10) (2017) 9614–9635.
[23] J. Kim, et al., Wearable biosensors for healthcare monitoring, Nat. Biotechnol. 37 (4) (2019) 389–406.
[24] S. Caras, J. Janata, Field effect transistor sensitive to penicillin, Anal. Chem. 52 (12) (1980) 1935–1937.
[25] S. Mao, et al., Two-dimensional nanomaterial-based field-effect transistors for chemical and biological sensing, Chem. Soc. Rev. 46 (22) (2017) 6872–6904.
[26] D. Rani, et al., Point-of-care-ready nanoscale ISFET arrays for sub-picomolar detection of cytokines in cell cultures, Anal. Bioanal. Chem. 412 (2020) 6777–6788.
[27] D. Rani, et al., Top-down fabricated silicon nanowire arrays for field-effect detection of prostate-specific antigen, ACS Omega 3 (8) (2018) 8471–8482.
[28] G. Figueroa-Miranda, et al., Delineating charge and capacitance transduction in system-integrated graphene-based BioFETs used as aptasensors for malaria detection, Biosens. Bioelectron. 208 (2022) 114219.
[29] O. Parlak, et al., Molecularly selective nanoporous membrane-based wearable organic electrochemical device for noninvasive cortisol sensing, Sci. Adv. 4 (7) (2018) eaar2904.
[30] G. Jeong, J. Oh, J. Jang, Fabrication of N-doped multidimensional carbon nanofibers for high-performance cortisol biosensors, Biosens. Bioelectron. 131 (2019) 30–36.
[31] X. Xu, et al., Reconfigurable carbon nanotube multiplexed sensing devices, Nano Lett. 18 (7) (2018) 4130–4135.
[32] H.R. Kim, et al., Group selective aptamers: broad-spectrum recognition of target groups in Cronobacter species and implementation of electrochemical biosensors as receptors, Biosens. Bioelectron. 246 (2024) 115843.
[33] B.H. Lee, S.H. Kim, M.B. Gu, Biosensors: aptamer Sensors, in: R. Narayan (Ed.), Encyclopedia of Sensors and Biosensors, 1st ed., Elsevier: Oxford, 2023, pp. 363–376.
[34] T.T.Q. Nguyen, et al., An IoT-based aptasensor biochip for the diagnosis of periodontal disease, Biosens. Bioelectron. 251 (2024) 116097.
[35] S.H. Kim, et al., Specific detection of avian influenza H5N2 whole virus particles on lateral flow strips using a pair of sandwich-type aptamers, Biosens. Bioelectron. 134 (2019) 123–129.
[36] S. Dalirirad, A.J. Steckl, Aptamer-based lateral flow assay for point of care cortisol detection in sweat, Sens. Actuators B Chem. 283 (2019) 79–86.
[37] R.E. Fernandez, et al., Disposable aptamer-sensor aided by magnetic nanoparticle enrichment for detection of salivary cortisol variations in obstructive sleep apnea patients, Sci. Rep. 7 (1) (2017) 17992.
[38] S. Jo, et al., Localized surface plasmon resonance aptasensor for the highly sensitive direct detection of cortisol in human saliva, Sens. Actuators B Chem. 304 (2020) 127424.
[39] A. Susloparova, et al., Investigation of ISFET device parameters to optimize for impedimetric sensing of cellular adhesion, Phys. Status Solidi A 211 (6) (2014) 1395–1403.
[40] X.T. Vu, et al., Top-down processed silicon nanowire transistor arrays for biosensing, Phys. Status Solidi A 206 (3) (2009) 426–434.
[41] A. Ortiz-Conde, et al., A review of recent MOSFET threshold voltage extraction methods, Microelectron. Reliab. 42 (4–5) (2002) 583–596.
[42] J. Zhou, J. Rossi, Aptamers as targeted therapeutics: current potential and challenges, Nat. Rev. Drug Discov. 16 (3) (2017) 181–202.
[43] K.M. Cheung, et al., Phenylalanine monitoring via aptamer-field-effect transistor sensors, ACS Sens. 4 (12) (2019) 3308–3317.
[44] N. Nakatsuka, et al., Aptamer–field-effect transistors overcome Debye length limitations for small-molecule sensing, Science 362 (6412) (2018) 319–324 (1979).
[45] Q. Liu, et al., Flexible multiplexed In2O3 nanoribbon aptamer-field-effect transistors for biosensing, iScience 23 (9) (2020).
[46] S. Kim, et al., Analysis of current drift on p-channel pH-Sensitive SiNW ISFET by capacitance measurement, Curr. Appl. Phys. 18 (2018) S68–S74.
[47] J.H. Jeon, W.J. Cho, Ultrasensitive coplanar dual-gate ISFETs for point-of-care biomedical applications, ACS Omega 5 (22) (2020) 12809–12815.